

Catalytic Performance and Kinetic Study in the Total Oxidation of VOC over Micro/Meso Porous Catalysts

*Parsafard, Nastaran***

Department of Applied Chemistry, Kosar University of Bojnord, North Khorasan, I.R. IRAN

Peyrovi, Mohammad Hasan; Valipour Shokoohi, Mehrdad

*Department of Petroleum Chemistry and Catalysis, Faculty of Chemistry and Petroleum Sciences,
University of Shahid Beheshti, Tehran, I.R. IRAN*

ABSTRACT: *The total oxidation of toluene at a wide temperature range (200–500 °C) over micro/meso porous platinumed catalysts has been investigated about activity, selectivity to CO₂ and CO, catalyst's stability versus coke deposition and reaction kinetics. Kinetic of toluene oxidation was measured under various oxygen and toluene pressures and also the effect of the reaction conditions on the catalytic performance was studied. For more study, two kinetic models have also been selected and tested to describe the kinetics for this reaction. The results show that the Langmuir-Hinshelwood model provides a good fit for the experimental data. The obtained results showed that Pt/HZSM-5(30)-HMS have a better ability than other catalysts for the oxidation reaction of toluene, such as maximum toluene conversion (>97%), high selectivity to CO₂ (100%), good catalytic stability against coke deposition and appropriate kinetic parameters.*

KEYWORDS: *Toluene oxidation; Kinetics; Conversion; Selectivity; Stability; Langmuir-Hinshelwood model.*

INTRODUCTION

A major class of air pollutants is Volatile Organic Compounds (VOCs). The origin of these compounds is generally industrial processes such as refineries and synthetic flavoring or painting factories. These compounds have harmful effects on the environment and human health [1-4]. Accordingly, in recent years, the removal of VOCs has found great significance. Among VOCs emitted from industrial activities, toluene has been listed as a priority pollutant due to its easily volatile into the air, large consumption and serious damage to human health and the environment [5].

There are a number of physical and chemical methods for eliminating VOCs [6] that the overall catalytic oxidation (or catalytic combustion) is one of the most important and cost-effective of these methods [7, 8]. One of the important advantages of this method is the preformation at a low temperature due to the use of catalysts. So the energy consumption and the formation of undesirable by-products (as dioxins and NO_x) are decreased in this process [3].

The parameters that can affect the catalyst activity and their resistance to poisoning are effective on

* To whom correspondence should be addressed.

+ E-mail: n-parsafard@kub.ac.ir

1021-9986/2018/5/19-29

11/\$/6.01

the choice of the catalyst for this reaction [8]. Different supported noble metals (Pt, Pd, Rh, Au, etc.) and metal oxides (CeO_2 , CuO, MnO_x , CoO_x , etc.) were used for total oxidation of VOCs [9]. Among these catalysts, noble-metal (especially Pd and Pt) supported catalysts have the highest activity. In these catalysts, the supports have an important effect on the generation of active species and on the catalytic performance [10]. According to literature [10], the acid-base properties of supports and the type of acids are very effective on the catalytic activity and the dispersion of active phase. Among the catalysts used for this reaction, HZSM-5 zeolite has the most favorable acidity and structural properties. The only disadvantage of this support is the small size of its pores. On the other hand, in recent years, many researchers have been made to design new catalysts based on mesoporous silica because of its potential uses as a matrix for better dispersion and so providing more active sites for the reaction. Although they have very little acidity, a good pore size and low diffusion limitations. Hexagonal Mesoporous Silica (HMS) is one of these mesoporous silica which has attracted a lot of attention in recent years.

In order to obtain materials that combine the advantages of mesoporous and microporous materials, we developed a new method for the preparation of micro/meso porous catalyst (HZSM-5/HMS) in our reported work [11]. These composite catalysts have a good property for the catalytic reaction. In this sense, the objective of the present report is a study of catalytic combustion of toluene, which is a typical volatile organic compound, on different Pt catalysts supported on HZSM-5/HMS materials, with different HZSM-5 contents. In the other word, we demonstrate that such composite catalysts can be effectively applied in VOC catalytic oxidation. For this purpose, the catalytic performances of these catalysts as activity, selectivity and stability and also kinetics of the toluene oxidation were reported in present work. Finally, we investigated the relationship between the catalytic activity and the structural properties of catalysts involving porous structure, acidity and other properties for deep oxidation of toluene.

EXPERIMENTAL SECTION

Catalyst preparation

The preparation procedure of platinated- HMS, HZSM-5 and HZSM5(x)/HMS catalysts is described

elsewhere in details [11]. In a nutshell, the HZSM5(x)/HMS supports were prepared by adding 10, 20, 30 and 40 wt% of commercial HZSM-5 (Zeolyst international, Si/Al = 14) with proportional values of ethanol, tetraethyl ortho silicate, dodecyl amine, HCl (1 M) and distilled water. After 6 h calcination of these materials at 600 °C, 0.6 wt.% of Pt was loaded on these materials. Finally, the solvent was evaporated and then these Pt-loaded solids were dried and calcined at 300 °C for 4 h. These catalysts after calcination were named Pt/HMS, Pt/HZSM-5 and Pt/ZH-x (ZH is HZSM5/HMS support and x is weight percent of HZSM-5) [11].

Catalyst characterization

The used methods for analyzing are similar to previously published report [11]. The information about these methods is summarized here. It should be noted that all of these analyzes were done after Pt impregnation and calcination of the samples. These methods are as follows;

X-ray fluorescence (XRF) was done with XRF-8410 Rh apparatus and 60 kV voltage.

X-ray diffraction (XRD) was recorded with X-PERT diffractometer utilizing Ni-filtered $\text{Cu } \alpha$ radiation, 45 kV voltage, 50 mA electric current, 0.06° 2θ -step and 1 s/step ramp.

TPD/TPR analyzer model 2900 Micromeritics equipped with a TCD sensor were used for H_2 chemisorption.

Fourier transform infrared (FT-IR) was obtained by a BOMEM FT-IR spectrophotometer model Arid-Zone TM, MB series in $400\text{--}4000 \text{ cm}^{-1}$ wave number range.

N_2 adsorption-desorption isotherms was obtained from ASAP-2010 micromeritics at 350 °C evacuation temperature for 10 h.

Temperature programmed desorption of NH_3 (NH_3 -TPD) at 25-800 °C was prepared from TPD/TPR analyzer model 2900 Micromeritics equipped with a TCD sensor, pure helium for pretreating (40 mL/min) at 600 °C for 1 h, and 10 °C/min heating ramp.

Fourier transform infrared of pyridine (Py-IR) was also recorded with Fourier-transform infrared spectrometer model Nicolet 170 SX, at 250 °C evacuation temperature and 10^{-2} Pa overnight.

Thermogravimetric/differential thermal analysis (TG/DTA) was done with STA503 M apparatus, 5 vol.%

O₂/N₂ gas mixture, 60 mL/min flow rate and a heating ramp of 10 °C/min at 25-800 °C temperature range.

Catalytic evaluation

Activity test

The activity of studied catalysts was tested for toluene oxidation in a tubular fixed bed flow reactor of quartz that operated in continuous mode at atmospheric pressure. Prior to the catalytic activity measurements, the reaction temperature of each catalyst (0.3 g) was increased from room temperature to 400 °C and then stayed for 2 h at this temperature in He flow to pretreat the powder catalysts. The feed gas consisted of oxygen stream (180 mL/min flow rate) and toluene (2 mL/h flow rate). Toluene was supplied by a liquid injector, controlled by a liquid flow controller, transported into the evaporator and flow as vapor into the system. To detect the reaction temperature, a thermocouple was placed inside the reactor at the catalyst bed level. The corresponding Gas Hourly Space Velocity (GHSV) was 17,000 h⁻¹. It should be noted that the reaction was performed at temperatures ranging from 200 to 500 °C, and the only primary products were toluene (Tu), H₂O, CO and CO₂. Other products were not detected under our experimental conditions. Gas analyzer (Delta 1600-L) was used for analyzing these reaction products into the outlet gas.

The reported results of conversion and selectivity in this work were calculated on the basis of the following equations;

$$\text{Conversion (\%)} = \frac{[Tu]_i - [Tu]_o}{[Tu]_i} \times 100 \quad (1)$$

$$\text{Selectivity (\%)} = \frac{[CO_2] \text{ or } [CO]}{[\text{Converted products}]_{\text{total}}} \times 100 \quad (2)$$

Where $[Tu]_i$ and $[Tu]_o$ are the toluene concentration in the inlet and outlet gas at different temperatures.

Stability test

In order to distinguish the stability of the prepared catalysts during the reaction test, a series of experiments has been performed under reaction time using the same conditions with activity test. For this purpose, 0.3 g of each catalyst was evaluated in terms of conversion and selectivity at 350 °C for 60 h on stream.

Kinetic test

To further evaluate the differences in the catalytic ability, kinetic study of toluene oxidation was performed over these catalysts at follow conditions as 200-500 °C temperature range, a varied flow rate of gaseous toluene from 1.5 to 3 mL/h and a varied O₂ flow rate of 60-240 mL/min.

RESULTS AND DISCUSSION

Structure

Since the used catalysts in this work have previously been studied in terms of structural characteristics by our group elsewhere [11], the results for these analyses will be briefly presented here. The results are as follows;

The powder XRD patterns of the calcined platinumed catalysts were shown in Fig. 1.

This figure shows the successful synthesis of composite catalysts. In all of these spectra, the peaks characteristic of the HMS (2θ=2.3°) and HZSM-5 (2θ=6–11° and 22–25°) phases are observed. As can be seen, adding the HZSM-5 reduces intensity of the HMS peak and broads it [11]. The crystallite size of platinum has been estimated from the XRD patterns, using the line broadening at half the maximum intensity (FWHM) of platinum reflection that its results [11] is summarized in Table 1.

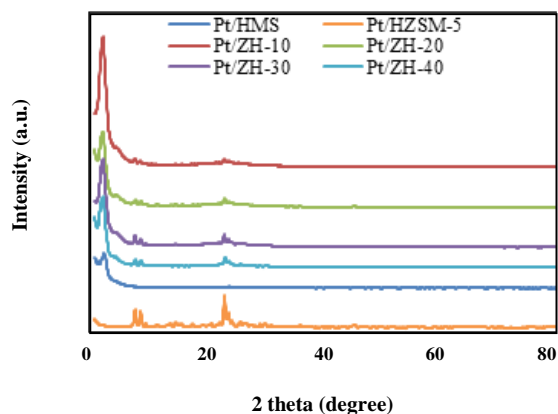
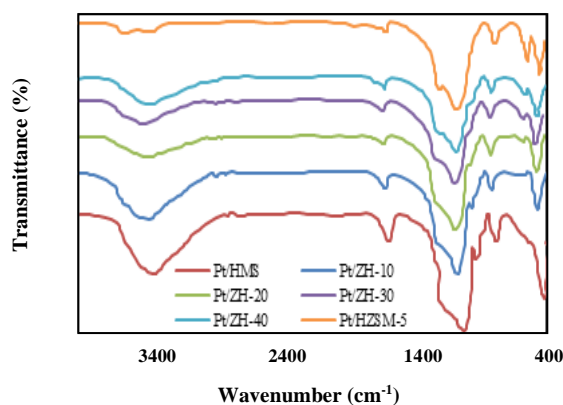
The prepared catalysts were also analyzed by FT-IR spectroscopy. Fig. 2 shows the infrared spectra for Pt-loaded HMS, HZSM-5 and ZH-x catalysts. In this figure, there are also multiple evidences for successful synthesis. They are as follows; The absorption bands at near 3436 cm⁻¹ that are related to the stretching vibrations of terminal Si–OH groups and adsorbed water molecules. The band at 1635 cm⁻¹ shows the hydroxyl of water vibrations. The bands at 1230, 1080 and 452 cm⁻¹ are related to the asymmetric stretching and bending modes of ≡Si–O–Si≡ for HMS. The asymmetric and symmetric stretching vibrations of framework Si–O–Si bonds of ZSM-5 are observed at 1024 and 812 cm⁻¹. The vibrations of the five- and six-membered rings of (Si or Al)–O–(Si or Al) in HZSM-5 and the tetrahedral Si–O bending mode have appeared at 554 cm⁻¹ and 453 cm⁻¹, respectively [10-12].

Fig. 3 demonstrates the NH₃-TPD profiles of Pt-supported catalysts in the range of 110–800 °C. The number of NH₃ molecules adsorbed per 1 g of each

Table 1: Physicochemical properties of the studied catalysts.

Catalysts	Pt/HMS	Pt/HZSM-5	Pt/ZH-10	Pt/ZH-20	Pt/ZH-30	Pt/ZH-40
Acid properties						
weak acid ^a	0.07	0.22	0.07	0.14	0.19	0.23
strong acid ^b	-	0.38	0.10	0.18	0.23	0.28
L+B ^c	0.07	0.60	0.17	0.32	0.42	0.51
B/L ^c	-	1.73	1.43	1.28	1.21	1.22
Surface properties						
S _{BET} (m ² /g) ^d	898	387	906	903	809	715
V _p (cm ³ /g) ^e	0.87	0.25	0.83	0.79	0.70	0.66
S _{micro} (m ² /g) ^d	-	311	29	59	96	124
V _{micro-p} (cm ³ /g) ^e	-	0.11	0.08	0.13	0.19	0.22
d _p (nm)	5.41	0.87	6.16	6.16	6.19	6.21
Si/Al ratio ^f	∞	14.01	69.10	63.35	57.22	51.40
Pt _d (%) ^g	71	73	75	81	92	84
Pt particle size (nm) ^h	1.58	1.53	1.49	1.38	1.22	1.33

^a at 230-250 °C versus mmol NH₃/g using NH₃-TPD method; ^b at 460-570 °C versus mmol NH₃/g using NH₃-TPD method; ^c Lewis and Brønsted acidity versus mmol Py/g using Py-IR method; ^d using BET isotherms; ^e using BJH method; ^f using XRF method; ^g using H₂ chemisorption; ^h using the line broadening at half the maximum intensity (FWHM) of platinum reflection.

**Fig. 1: XRD patterns of the prepared catalysts.****Fig. 2: FT-IR spectra for the KBr pellets of the prepared catalysts.**

catalyst obtained from this test, was summarized in Table 1. These results show the amounts of acidity. The weak acidic sites (the peak below 300 °C), the strong acidic sites (the peak located at 460-570 °C) and the peak above 700 °C about H₂O desorption were observed in Fig. 3.

This figure presents that the number of acid sites of ZH-x increases with increasing HZSM-5. The order of acidity is: Pt/HZSM-5 > Pt/ZH-40 > Pt/ZH-30 > Pt/ZH-20 > Pt/ZH-10 > Pt/HMS. The results in Table 1 show that the amount of strong acid sites on the ZH-x samples is much

higher than that of the pure HMS and is much smaller than that of the HZSM-5 sample [11].

The FT-IR spectra of pyridine (Py-IR) adsorption (Fig. 4) were used to identify the type of acid sites (Lewis and Brönsted). This figure reveals three peaks at ca 1449 and 1540 cm^{-1} due to pyridine adsorbed on Lewis (L) and Brönsted (B) acid sites, respectively and near 1480 cm^{-1} corresponded to Lewis and Brönsted sites [11]. It is observed that the intensities of Lewis and Brönsted bands increase with increasing of HZSM-5 content. The order of B/L ratios is as follows. Pt/HZSM-5 > Pt/ZH-10 > Pt/ZH-20 > Pt/ZH-40 > Pt/ZH-30 > Pt/HMS. It seems that the tetrahedrally coordinated framework aluminum (potential Brönsted acid site) and octahedrally extra framework aluminum (potential Lewis acid site) increase with increasing HZSM-5 content [11].

The nitrogen adsorption/desorption isotherms of platinated catalysts were shown in Fig. 5.

The results of these isotherms show that the surface areas of these catalysts change between 715 and 906 m^2/g (Table 1). Also the textural properties of these catalysts in Table 1 show that the pore volume (V_p) and pore size (d_p) increase with decreasing of the HZSM-5 amount that are corresponding to the decrease of micropore surfaces (S_{micro}) and micropore volumes ($V_{\text{micro-p}}$). In addition, compared with the results of the previous work [11], when platinum is impregnated on the supports, the lower surface areas are obtained. It seems that the incorporation of Pt blocks the pores and decreases partially structural ordering of the channels. Therefore, the decrease in the surface areas and pore volumes of supports was not unexpected reality.

In addition to the above analyzes, the Si/Al ratios and Pt contents in the prepared catalysts were calculated by XRF method. This analysis was done after impregnation of platinum and calcination of catalysts. The results of XRF analysis presented that the metal contents in close agreement with the expected theoretical ones for all catalysts (Table 1). The dispersion of platinum (Pt_d) was measured by the hydrogen adsorption method. The results show a great dispersion over composite catalysts for platinum compared to the initial value of platinum. Table 1 presents a summary of useful information to draw conclusions about the behavior of these catalysts.

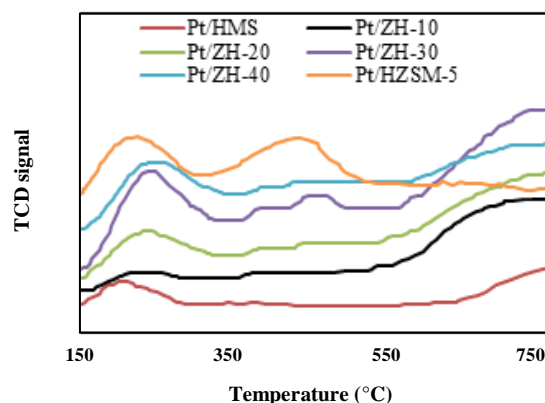


Fig. 3: NH_3 -TPD profiles for platinated catalysts.

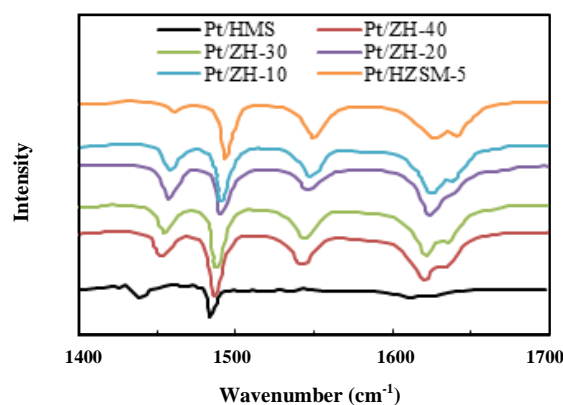


Fig. 4: IR spectra of adsorbed pyridine for different samples.

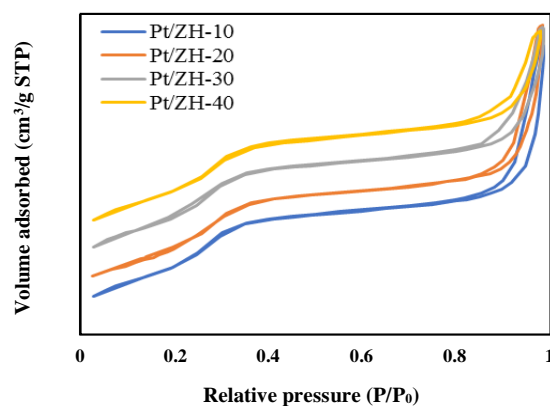


Fig. 5: N_2 adsorption and desorption isotherms of Pt-HZSM5/HMS composite catalysts.

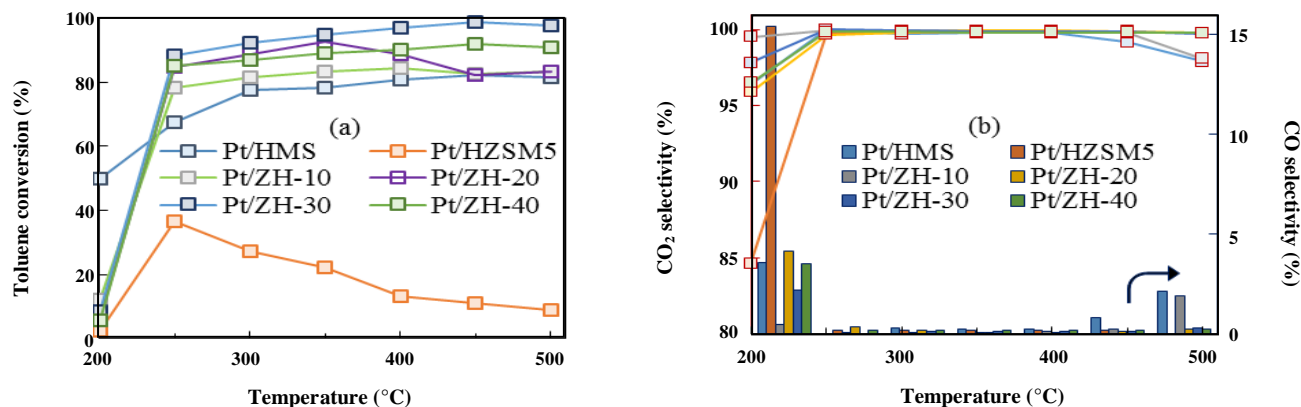


Fig. 6: (a) Toluene conversion and (b) catalytic selectivity to CO₂ and CO as a function of the reaction temperature.

Catalytic performance

Activity test

The activity results of Pt/ZH-*x* catalysts for toluene oxidation were shown in Fig. 6 a by the conversion in the range of 200–500 °C.

For the comparison, the conversion results of Pt/HMS and Pt/HZSM-5 catalysts have also been included in this figure. The reaction products in all cases were CO₂, CO and water. It can be clearly observed that the micro/meso porous composite catalysts show a higher conversion than Pt/HMS and Pt/HZSM-5 catalysts, achieving high conversion of toluene at temperatures over 250 °C. The order of the activity observed is: Pt/ZH-30 > Pt/ZH-40 > Pt/ZH-20 > Pt/ZH-10 > Pt/HMS > Pt/HZSM-5 for toluene conversion. However, Pt/HMS, Pt/ZH-10 and Pt/ZH-20 catalysts do not follow this trend at 500 °C and show the same conversion. Toluene conversion for all prepared catalysts increases with increasing temperature except Pt/HZSM-5 and Pt/ZH-20 that it can be related to the deactivation of these catalysts by coking at high temperatures.

Furthermore, a comparison of the CO and CO₂ selectivity in the toluene oxidation as a function of the reaction temperature for all catalysts was shown in Fig. 6 b. Over the whole temperature range, the prepared catalysts show approximately the same trend. The results show that the CO₂ generation rate is very close to the toluene conversion rate, and the selectivity to CO₂ and CO is near to 100% and around zero, respectively.

Stability test and coke formation

In the oxidation reaction of VOCs, due to the use of aromatic compounds, the carbonaceous deposits (coke) are formed upon the catalyst surfaces.

The carbonaceous deposits, mainly led to the loss of the catalytic activity during the oxidation reaction. Therefore, the stability of catalysts is critical in this reaction. Accordingly, the stability test was carried out continuously at 350 °C for more than 60 h. The important observation about Pt/HZSM-5(*x*)-HMS catalysts (Fig. 7) is that the catalytic activity remains relatively stable for the used catalyst. The spent catalysts were gray color due to a different coke deposition. Coke burning from the spent catalysts by ThermoGravimetric Analysis (TGA) released considerable amounts of the deposited coke. The results show that loading different HZSM-5 contents onto the similar catalytic supports would lead to the significant difference in the coke formation (4–10 wt%). The greatest and the lowest amounts of coke formed on Pt/HZSM-5 (10 wt%) and Pt/ZH-30 (4 wt%), respectively. The observed order in relation to the formation of coke is as follows; Pt/HZSM-5 > Pt/ZH-20 > Pt/ZH-10 > Pt/ZH-40 > Pt/HMS > Pt/ZH-30. According to the reported data in Table 1, it seems that the formation of coke is influenced by the ratio of two types of acid sites (B/L ratio). However, the interaction of other factors, such as Pt dispersion and surface area, is undeniable.

Kinetic study

To ensure that the diffusion limitations do not effect on the obtained results, the Koros-Nowak [13] and Madon-Boudart [14] tests were performed with seven different amounts of catalyst from 0.3 to 1.2 g. The results show that in the weights over 1.0 g of catalyst, the reaction is affected by a diffusion regime (Fig. 8 a). To avoid this effect, it is appropriate to use a catalyst bed

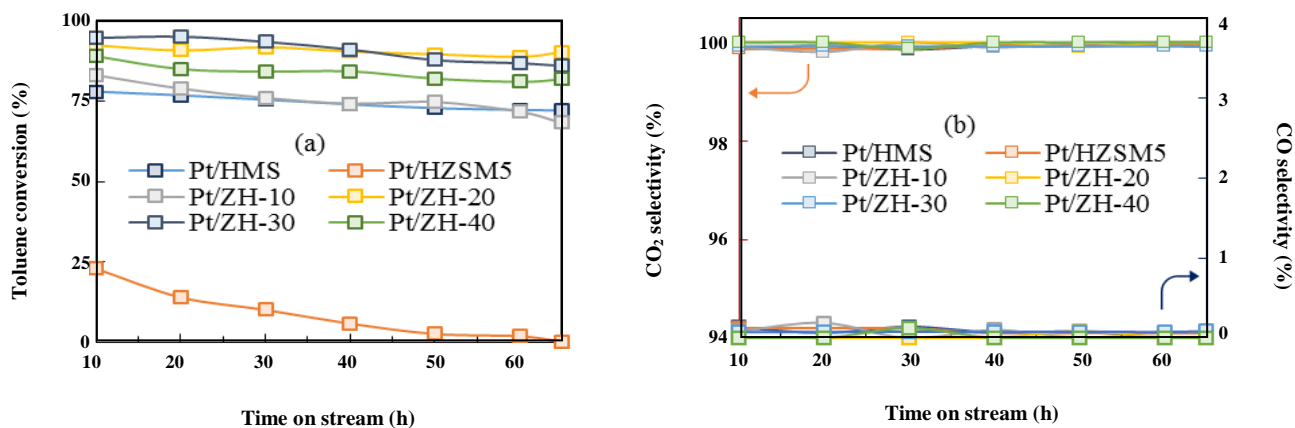


Fig. 7: (a) Toluene conversion and (b) catalytic selectivity to CO₂ and CO as a function of the reaction time for the prepared catalysts.

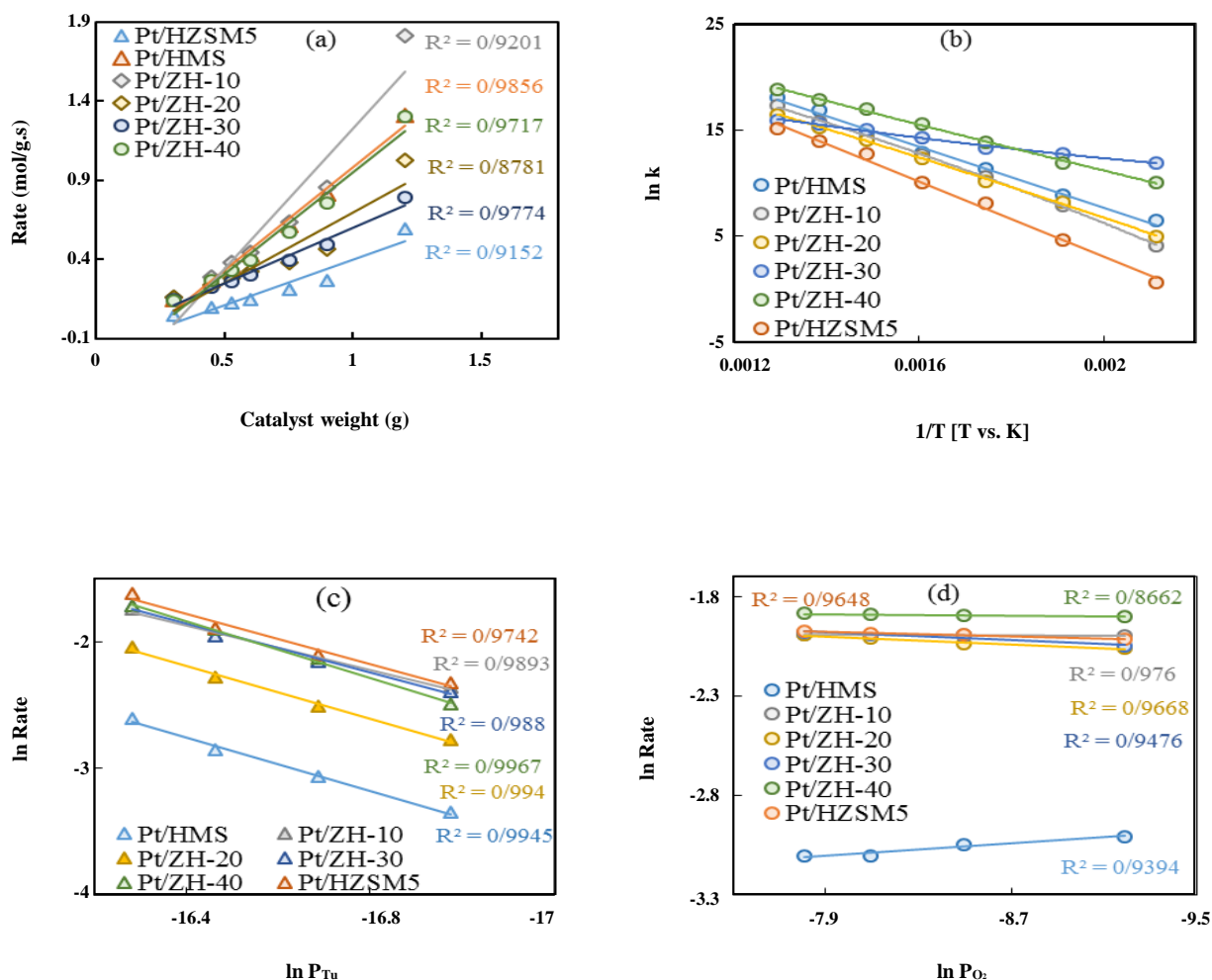


Fig. 8: (a) Effect of diffusion regime on the oxidation reaction of toluene at 350 °C, (b) Arrhenius plots and (c, d) double-log plots of the reaction rate for VOCs oxidation versus the partial pressures of toluene and oxygen at 350 °C, respectively.

containing 1.0 g of catalyst or less. We also observed that the results of these tests deviated from straight line at high temperatures, especially at 500 °C, indicating the effect of the diffusion limitations at this temperature.

To study the reaction kinetics of catalysts and provide a reaction mechanism, the rates of this process were measured as a function of temperature (200-500 °C) in a flow rate range of toluene (1.5–3.0 mL/h) and oxygen (60-240 mL/min). For the calculation of kinetic parameters, we used the following equations;

$$r\left(\frac{\text{mol}}{\text{g.s}}\right) = \frac{\text{Toluene flow rate}\left(\frac{\text{mL}}{\text{s}}\right) \cdot \text{Toluene density}\left(\frac{\text{g}}{\text{mL}}\right) \cdot \text{conversion}(\%)}{\text{Toluene molar weight}\left(\frac{\text{g}}{\text{mol}}\right) \cdot \text{weight of catalyst (g)} \cdot \text{impregnated metal (wt\%)}} \quad (3)$$

and also the power law;

$$r\left(\frac{\text{mol}}{\text{g.s}}\right) = k P_{\text{O}_2}^n P_{\text{Tu}}^m \quad (4)$$

In this reaction, n and m are the partial orders of oxygen and toluene respectively, and k is the rate constant and determined by below equation.

$$k = A \exp\left(-\frac{E_{\text{app}}^{\text{act}}}{RT}\right) \quad (5)$$

where A is Arrhenius constant.

To obtain the reaction orders, linear fits of double-log plots were measured by varying the partial pressures of O₂ and Tu at different temperatures (Fig. 8 c, d). To draw these plots, a series of reaction feeds containing various injection rates of toluene (1.5-3.0 mL/h flow rate) with a constant flow rate of O₂ at 180 mL/min was measured at a constant temperature within the range of 200-500 °C. The next step was done as first step with varying the oxygen flow rate (60-240 mL/min) and 2 mL/h flow rate of toluene. The slopes of these plots were used as the partial reaction orders of toluene and oxygen, respectively.

The plots of $\ln K$ vs. $1/T$ calculated from the experimental kinetic data have also studied for different conditions (Fig. 8 b). The correlation coefficients (R^2) for the Arrhenius plots are above 0.9. Table 2 summarizes the apparent activation energies ($E_{\text{app}}^{\text{act}}$) and the reaction

orders of Tu and O₂ calculated for the total oxidation of toluene in the gas phase using the Power Law (PL) model.

The reaction orders for toluene and oxygen on the prepared catalysts at a constant temperature were measured 0.7-1.2 and -0.6 to 0.1, respectively. These results are in fairly good agreement with literature data [8, 15-17]. The negative orders were observed at low temperatures that indicate self-inhibition on the catalysts. As it can be seen in this table, the reaction orders of O₂ and toluene increase almost with reaction temperature, probably due to a substantial decrease in the coverage of each reactant. The lowest and highest calculated activation energies are 42.4 and 147.1 kJ/mol for Pt/ZH-30 and Pt/HZSM-5, respectively. The activation energy for Pt/ZH-30 was calculated better than the reported activation energies for complete combustion of hydrocarbons [15-17] that confirms the reaction rate on this catalyst is more than others. The results of the calculated vs. the experimental Tu conversion were shown in Fig. 9 a. This figure presents a fairly good agreement between the experimental and the calculated data. Although the PL model is only mathematical model and does not have a direct connection with the reaction mechanism, its kinetic results are similar to those reported in the literature [15-17].

Several other kinetic models were used to describe the kinetic of the catalytic oxidation of toluene over various catalysts [18]. One of these kinetic models is Langmuir–Hinshelwood (LH) mechanism that the reaction takes place between adsorbed species on the catalyst surface. According to literature [18, 19], if the rate determining step is the surface reaction between adsorbed toluene and adsorbed molecular oxygen on similar type of active sites, the rate equation will be as follows;

$$-r = \frac{k \cdot k_{\text{Tu}} \cdot P_{\text{Tu}} \cdot k_{\text{O}_2} \cdot P_{\text{O}_2}}{(1 + k_{\text{Tu}} \cdot P_{\text{Tu}} + k_{\text{O}_2} \cdot P_{\text{O}_2})^2} \quad (6)$$

where k is the rate constant and k_{O_2} and k_{Tu} are the rate constants of O₂ and Tu adsorptions, respectively. In this equation, it was assumed that the adsorption constants (k_{O_2} and k_{Tu}) follow a Van't Hoff type equation.

$$k_x = A_x e^{\frac{\Delta H_{\text{ads-x}}}{RT}} \quad (7)$$

Table 2: Kinetic parameters at various temperatures for the VOCs oxidation.
(n_{O_2} and m_{Tu} are the partial reaction orders for oxygen and toluene, respectively).

Temp.	orders	Pt/HMS	Pt/HZSM-5	Pt/ZH-10	Pt/ZH-20	Pt/ZH-30	Pt/ZH-40
Power law model							
200 °C	n_{O_2}	-0.2	-0.2	-0.5	-0.2	-0.2	-0.6
250 °C	n_{O_2}	-0.2	0.0	-0.3	-0.2	0.0	-0.1
300 °C	n_{O_2}	-0.1	0.0	0.0	0.0	0.0	0.0
350 °C	n_{O_2}	-0.1	0.0	0.0	0.0	0.0	0.0
400 °C	n_{O_2}	-0.0	0.0	0.0	0.1	0.0	0.1
450 °C	n_{O_2}	0.0	0.0	0.1	0.1	0.0	0.1
500 °C	n_{O_2}	0.0	0.0	0.1	0.1	0.0	0.1
200 °C	m_{Tu}	0.7	1.1	0.8	0.7	0.9	1.0
250 °C	m_{Tu}	0.7	1.1	0.8	0.9	1.0	1.0
300 °C	m_{Tu}	1.0	1.0	0.9	1.0	1.0	1.1
350 °C	m_{Tu}	1.0	1.0	0.9	1.0	1.0	1.1
400 °C	m_{Tu}	1.1	1.0	0.9	1.0	1.0	1.1
450 °C	m_{Tu}	1.1	1.0	1.0	1.0	1.0	1.1
500 °C	m_{Tu}	1.2	1.0	1.1	1.1	1.1	1.2
E_{app}^{act} (kJ/mol)		118.5	147.1	130.6	115.4	42.4	90.6
R ² value		0.92	0.89	0.88	0.89	0.89	0.92
Langmuir-Hinshelwood model							
K	E_{app}^{act} (kJ/mol)	84.1	136.1	88.6	42.8	23.0	27.8
	A (mol/gs)	3.9×10^{-28}	2.9×10^{-25}	1.0×10^{-25}	1.9×10^{-20}	2.9×10^{-14}	8.4×10^{-19}
K_{Tu}	ΔH_{ads-Tu} (kJ/mol)	-4.9	-5.5	-4.9	-4.9	-4.9	-4.9
	A_{Tu} (atm ⁻¹)	64.9	57.1	64.9	64.9	64.9	64.9
K_{O_2}	ΔH_{ads-O_2} (kJ/mol)	-63.1	-44.6	-25.8	-28.3	-19.8	-31.9
	A_{O_2} (atm ⁻¹)	3.9×10^7	3.8×10^8	2.8×10^{10}	9.2×10^{10}	9.4×10^{11}	2.7×10^{10}
R ² value		0.99	0.99	0.98	0.99	0.99	0.99

Eq. (6) can be expanded by Eq. (5) and Eq. (7).

$$-r = \frac{\left(A e^{-\frac{E_{app}^{act}}{RT}} \right) \cdot \left(A_{Tu} e^{-\frac{\Delta H_{ads-Tu}}{RT}} \right) \cdot P_{Tu} \cdot \left(A_{Tu} e^{-\frac{\Delta H_{ads-O_2}}{RT}} \right) \cdot P_{O_2}}{\left(1 + \left(A_{Tu} e^{-\frac{\Delta H_{ads-Tu}}{RT}} \right) \cdot P_{Tu} \cdot \left(A_{Tu} e^{-\frac{\Delta H_{ads-O_2}}{RT}} \right) \cdot P_{O_2} \right)} \quad (8)$$

The pre-exponential factors, activation energies and heats of adsorption can be estimated with a numerical

method. The kinetic parameters in these models were estimated by numerical integrations in order to obtain the best fit between experimental data and the calculated rate equation. The kinetic parameters of Eq. (8) have been estimated and listed in Table 2. These results show that the activation energies calculated via the LH model are lower than the activation energies measured by the PL model. This observation is probably due to the simplicity of PL model and the lack of consideration of the O₂ and Tu adsorptions in the PL model.

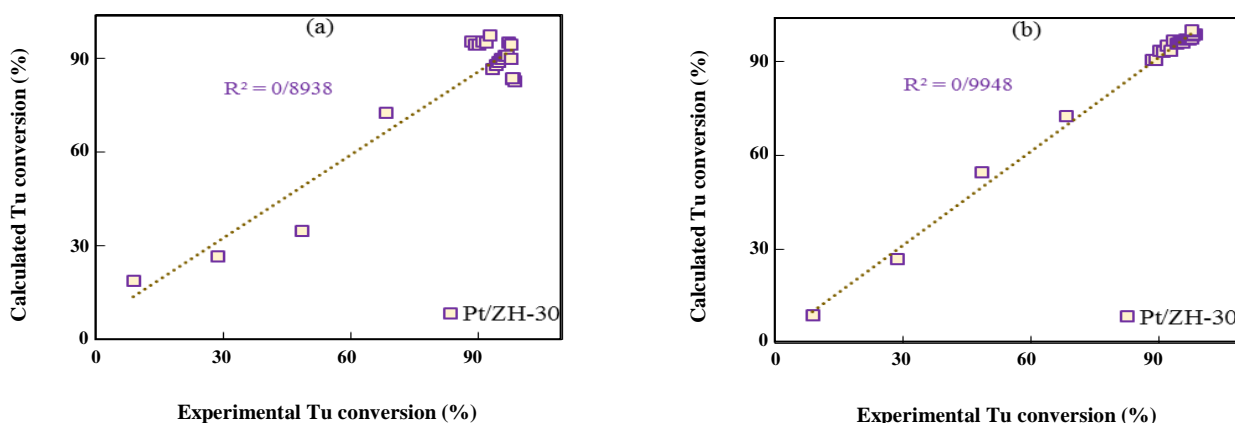


Fig. 9: (a) Estimated data by power law model and (b) estimated data by Langmuir-Hinshelwood model.

The negative values for the adsorption heats of Tu and O₂ were observed in Table 2. These data show the exothermic nature of this reaction. The pre-exponential factor of adsorption for O₂ (A_{O_2}) is higher than that of the Tu (A_{Tu}). This higher values probably indicate faster and stronger adsorption of O₂ over the surface of these catalysts. The kinetic parameters of LH model were used to simulate the Tu conversion for different prepared catalysts. Fig. 9 b represents the results of the calculated Tu conversion by LH model vs. the conversion obtained experimentally. The results of this model fit accurately the experimental data.

According to the obtained results of these two models, the PL model presents less accuracy than the LH model. This is probably because of the power law has a simpler expression in terms of numerical adjustment and does not consider the surface interactions and the mechanism of reactions.

CONCLUSIONS

In this work, we have used the Pt supported catalysts over micro/meso porous materials in the total oxidation of toluene. This process was studied in 200-500 °C temperature range. Using the previously published characterization data and obtained results, it can be briefly concluded as below.

The catalytic acidity is affected by the HZSM-5 content. It is clearly observed that the acidity and strength of acid sites are directly related to this content and increases almost linearly with the HZSM-5 amount. Among the prepared catalysts, Pt/ZH-10 has the best surface area. It can be seen with increasing HZSM-5

amount, the surface area of prepared catalysts decreases. There is no clear trend in the Pt distribution and the best Pt distribution is observed for Pt/ZH-30.

From the obtained results, it can be concluded that the best catalytic behavior was observed for platinated composite catalysts, especially Pt/ZH-30, with high toluene conversion (>97% at T=200-500 °C), the highest CO₂ selectivity (100%) and the low coke formation (4 wt%). The results show that the Tu conversion is affected by the Pt dispersion and the coke deposition is influenced by the B/L ratios.

According to the Koros-Nowak and Madon-Boudart tests, the rate of toluene oxidation reaction under experiment conditions is controlled by the intrinsic reaction kinetics and is free from transport limitations. Two kinetic models (power law and Langmuir-Hinshelwood) were tested in the kinetic study by estimating kinetic parameters and then simulating conversion data to be compared to experimental data, in order to validate the model. The obtained results show that the Tu oxidation is well described by the Langmuir-Hinshelwood model, suggesting is as the reaction mechanism. The best activation energy was also found 42.4 kJ/mol (PL model) and 23.0 kJ/mol (LH model) for Pt/ZH-30 catalyst indicates that the oxidation reaction on this catalyst is more convenient than other catalysts.

Acknowledgments

The authors greatly thank the financial support of the Iran National Science Foundation (project number 96003303). Grateful thanks also go to the Research Center for Oil and Gas Exploration of Shahid Beheshti University.

Received : Jan. 18, 2017 ; Accepted : Oct. 30, 2017

REFERENCES

- [1] Li Y., Fan Z., Shi J., Liu Z., Zhou J., Shangguan W., Removal of Volatile Organic Compounds (VOCs) at Room Temperature using Dielectric Barrier Discharge and Plasma-Catalysis, *Plasma Chem. Plasma Process.*, **34**(4): 801-810 (2014).
- [2] Darracq G., Couvert A., Couriol C., Amrane A., Le Cloirec P., Removal of Hydrophobic Volatile Organic Compounds in an Integrated Process Coupling Absorption and Biodegradation—Selection of an Organic Liquid Phase, *Water, Air, Soil Pollut.*, **223**(8): 4969-4997 (2012).
- [3] Abdelouahab-Reddam Z., El Mail R., Coloma F., Sepúlveda-Escribano A., Effect of the Metal Precursor on the Properties of Pt/CeO₂/C Catalysts for the Total Oxidation of Ethanol, *Catal. Today.*, **249**: 109-116 (2015).
- [4] Wang G., Dou B., Zhang Z., Wang J., Liu H., Hao Z., Adsorption of Benzene, Cyclohexane and Hexane on Ordered Meso Porous Carbon, *J. Env. Sci.*, **30**: 65-73 (2015).
- [5] Liang X., Qi F., Liu P., Wei G., Su X., Ma L., He H., Lin X., Xi Y., Zhu J., Zhu R., Performance of Ti-Pillared Montmorillonite Supported Fe Catalysts for Toluene Oxidation: The Effect of Fe on Catalytic Activity, *Appl. Clay Sci.*, **132**: 96-104 (2016).
- [6] Lee S., Choi I., Chang D., Multi-Objective Optimization of VOC Recovery and Reuse in Crude Oil Loading, *Appl. Energy*, **108**: 439-447 (2013).
- [7] Ali A., Hira Zafar M. Z., ul Haq I., Phull A. R., Ali J. S., Hussain A., Synthesis, Characterization, Applications, and Challenges of Iron Oxide Nano Particles, *Nanotechnol. Sci. Appl.*, **9**: 49-67 (2016).
- [8] Behar S., Gómez-Mendoza N. A., Gómez-García M. Á., Świerczyński D., Quignard F., Tanchoux N., Study and Modelling of Kinetics of the Oxidation of VOC Catalyzed by Nanosized Cu–Mn Spinel Prepared via an Alginate Route, *Appl. Catal. A. Gen.*, **504**: 203-210 (2015).
- [9] Abdelouahab-Reddam Z., El Mail R., Coloma F., Sepúlveda-Escribano A., Platinum Supported on Highly-Dispersed Ceria on Activated Carbon for the Total Oxidation of VOCs, *Appl. Catal. A. Gen.*, **494**: 87-94 (2015).
- [10] He, C., Li, P., Cheng, J., Wang, H., Li, J., Li, Q., Hao, Z., Synthesis and Characterization of Pd/ZSM-5/MCM-48 biporous Catalysts with Superior Activity for Benzene Oxidation, *Appl. Catal. A. Gen.*, **382**(2): 167-175 (2010).
- [11] Parsafard N., Peyrovi M. H., Rashidzadeh M., n-Heptane Isomerization on a New Kind of micro/meso Porous Catalyst: Pt Supported on HZSM-5/HMS, *Micropor. Mesopor. Mater.*, **200**: 190-198 (2014).
- [12] Li X., Li B., Xu J., Wang Q., Pang X., Gao X., Zhou Z., Piao J., Synthesis and Characterization of Ln-ZSM-5/MCM-41 (Ln= La, Ce) by Using Kaolin as Raw Material, *Appl. Clay Sci.*, **50**: 81-86 (2010).
- [13] Koros R. M., Nowak, E. J., A Diagnostic Test of the Kinetic Regime in a Packed Bed Reactor, *Chem. Eng. Sci.*, **22**: 470 (1967).
- [14] Madon, R. J., Boudart, M., Experimental Criterion for the Absence of Artifacts in the Measurement of Rates of Heterogeneous Catalytic Reactions, *Ind. Eng. Chem. Fund.*, **21**: 438-447 (1982).
- [15] Masui T., Imadzu H., Matsuyama N., Imanaka N., Total Oxidation of Toluene on Pt/CeO₂–ZrO₂–Bi₂O₃/γ-Al₂O₃ Catalysts Prepared in the Presence of Polyvinyl Pyrrolidone, *J. Hazard. Mater.*, **176**(1): 1106-1109 (2010).
- [16] Berenjian A., Chan N., Malmiri H. J., Volatile Organic Compounds Removal Methods: A Review, *Am. J. Biochem. Biotechnol.*, **8**(4): 220-229 (2012).
- [17] Huang H., Xu Y., Feng Q., Leung D. Y., Low Temperature Catalytic Oxidation of Volatile Organic Compounds: A Review, *Catal. Sci. Tech.*, **5**(5): 2649-2669 (2015).
- [18] Kamal, M. S., Razzak, S. A., Hossain, M. M., Catalytic Oxidation of Volatile Organic Compounds (VOCs)—A Review, *Atmos. Env.*, **140**: 117-134 (2016).
- [19] Bedia, J., Rosas, J. M., Rodríguez-Mirasol, J., Cordero, T., Pd Supported on Mesoporous Activated Carbons with High Oxidation Resistance as Catalysts for Toluene Oxidation, *Appl. Catal. B: Env.*, **94**(1): 8-18 (2010).